Peptide Design

DOI: 10.1002/anie.201107894

Bio-Inspired Design and Potential Biomedical Applications of a Novel Class of High-Affinity Peptides**

*Sunghyun Kim, Daejin Kim, Hyun Ho Jung, In-Hyun Lee, Jae IL Kim, Jeong-Yong Suh, and Sangyong Jon**

Antibodies have been widely used in a range of biopharmaceutical and biomedical applications due to their intrinsic high affinity and specificity toward various targets.[1] However, poor tissue penetration owing to their large size, undesired effector functions, immunogenicity, costly recombinant production in mammalian cells, and complex intellectual property barriers (royalty stacking) have led researchers to seek alternatives to antibodies.[2] Protein-scaffold-based affinity molecules[3] and oligo DNA or RNA-based aptamers[4] have recently emerged as novel high-affinity molecules that have indeed demonstrated potential utility in diagnosis and therapy. A common feature of such high-affinity molecules is that they possess three-dimensional folded structures that facilitate target binding through a large recognition interface, resulting in tight target binding with high specificity. High-affinity molecules with small molecular mass exhibit rapid extravasation and higher tissue penetration than bigger high-affinity molecules[5] and can be used as cancer diagnostics[6] or therapeutics.[7] To date, however, few reports have described the development of peptide-scaffold-based affinity molecules, presumably because it is difficult for peptides to form robust pre-organized structures. The knottin family[8] and phylomers[9] are peptide scaffolds engineered from naturally occurring protein domains; tight peptide binders with micromolar[10] or nanomolar affinities[11] can be selected from these two families. However, multiple disulfide bonds are involved in stabilizing knottin scaffolds. Thus, structural determination is necessary to ensure assumption of the correct fold, which limits the speed of product development.[12] Phylomers are not peptide scaffolds with a defined, single structural framework; they rather consist of a library of diverse naturally occurring structural frameworks derived from foreign sources. Therefore, the structures of selected 'hits' must be solved to figure out the specific scaffold, and there is a concern on potential immunogenicity because of the origin of phylomers.[9]

To our knowledge, no reports have described artificial peptide scaffolds that can be used as a general source of high-affinity peptides and that exhibit affinities toward a variety of biological targets in the nanomolar range. An artificial peptide scaffold must satisfy the following design criteria: 1) it should be able to form a secondary structure; 2) its pre-organized structure should be stable and robust; 3) it should have a sufficient number of variable (randomizable) amino acids to create diversity; and 4) its variable regions should minimally affect its secondary structure.

Herein, inspired by the structure of basic leucine zipper (bZIP) proteins, which function as transcriptional regulators in all eukaryotes through high-affinity (ca. low nanomolar), sequence-specific recognition of unique DNA motifs, we rationally designed novel artificial peptide-scaffold-based affinity molecules that form robust pre-organized structures and are capable of binding targets with high affinity and specificity. Homo- or heterodimeric bZIP proteins have a basic region that abuts a sequence of hepta-leucine repeats (Figure 1 a). The upper leucine-zipper region serves as a scaffold that maintains a unique open-mouthed structure through which variable basic regions are used to recognize DNA sites.[13] Exploiting these features, we designed new artificial high-affinity peptide ligands, which we have termed "aptides", from aptamer-like peptides. An aptide comprises a stabilizing scaffold and two target-binding regions (Figure 1 a). The scaffold consists of a small (12 amino acids) but highly stable tryptophan zipper (trpzip; $T_m = 72\,^{\circ}C$) that forms a leucine-zipper-like β-hairpin structure, in which two tryptophan–tryptophan cross-strand pairs create a robust and stable structure.[14] To mimic the DNA recognition site of bZIP proteins two target-binding regions, each comprising six randomizable amino acids, are introduced at both ends of the trpzip scaffold through glycine linkers. We expected that aptides would bind their target molecules with high affinity and specificity as a result of the synergistic action of the two target-binding sites.

We used phage display to explore the feasibility of using aptide libraries as a source of high-affinity peptide candidates for screening against protein targets. For functional selection, the aptide libraries were adapted for monovalent display on filamentous bacteriophage surfaces. As an initial target protein for evaluating the aptide platform, we chose human fibronectin extradomain B (EDB), which is a validated tumor-specific biomarker that has been used in tumor imaging and therapy.[15] Phage-display-based selections of the aptide library (8×10^8) against biotinylated EDB bound to

[*] S. Kim, D. Kim, H. H. Jung, I.-H. Lee, Prof. J. I. Kim, Prof. S. Jon
School of Life Sciences
Gwangju Institute of Science and Technology (GIST)
123 Cheomdangwagi-ro, Gwangju 500-712 (South Korea)
E-mail: syjon@gist.ac.kr
Prof. J.-Y. Suh
Biomodulation Major, Department of Agricultural Biotechnology
Seoul National University
1 Gwanak-ro, Seoul 151-921 (South Korea)

[**] This work was supported by a grant from the National Research Foundation of Korea (NRF), MEST (grant number: 20110000143) and by a grant from Cell Dynamics Research Center, KOSEF (grant number: 20110001163).

Supporting information for this article is available on the WWW under http://dx.doi.org/10.1002/anie.201107894.

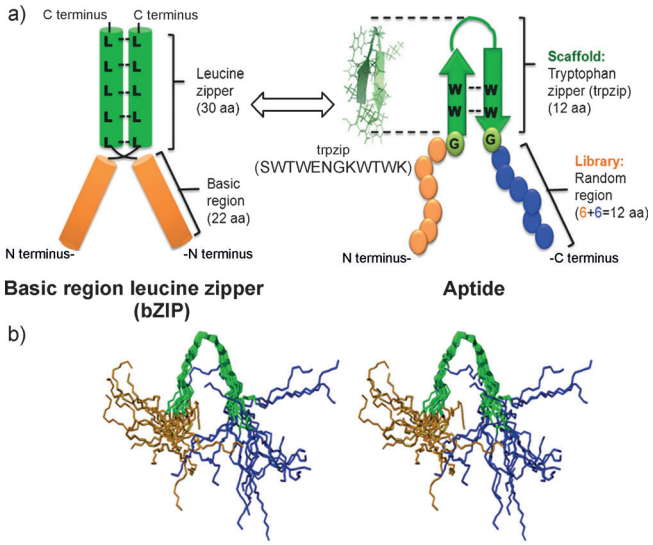

Figure 1. a) Design rationale of an aptide. Structural comparison between the basic region leucine zipper (bZIP) motif (left) and an aptide (right). The leucine zipper contains interacting hepta-leucine (L) repeats and serves as a stable scaffold, while the basic regions are capable of recognizing unique DNA sites with high affinity. Similarly, the aptide has a trpzip (green) region with tryptophan–tryptophan (W–W) cross-strand pairs as a scaffold and two randomized ligand-binding regions (orange and blue) that are capable of synergistically binding the target. Each orange or blue circle in the aptide represents a randomized amino acid, while the green circles denote the glycine linkers connecting the scaffold to the randomized binding sites. A ribbon diagram of a trpzip structure is included (protein database ID 1 LE1). b) NMR structures of an aptide. Stereopairs of backbone atoms (N, C^{α}, C) for twenty converged NMR structures obtained from a model aptide (APT_{EDB}). The N-terminal randomized region, the C-terminal randomized region and the trpzip scaffold are shown in orange, blue, and green, respectively.

Table 1: Kinetic binding data for selected aptides, as determined by affinity measurements using BIAcore chips adapted for surface plasmon resonance.

Target	Aptide name	k_a [$M^{-1}s^{-1}$]	k_d [s^{-1}]	K_d [M]
EDB	APT_{EDB}	1.7×10^{4}	1.1×10^{-3}	65×10^{-9}
EDB	APT_{EDB}^{1st}	3.0×10^{4}	5.1×10^{-4}	16×10^{-9}
EDB	APT_{EDB}^{2nd}	1.3×10^{4}	4.7×10^{-4}	3×10^{-9}
VEGF	APT_{VEGF}	3.5×10^{5}	1.0×10^{-2}	30×10^{-9}
CD7	APT_{CD7}	1.4×10^{5}	1.3×10^{-2}	93×10^{-9}
His_6-tag	$APT_{His\text{-}tag}$	5.3×10^{4}	3.7×10^{-3}	71×10^{-9}

EDB: human fibronectin extradomain B, VEGF: human vascular endothelial growth factor, CD7: human cluster of differentiation 7.

a streptavidin plate yielded enrichment of bound phages after the third round of selection (Figures S1a and S1b in the Supporting Information). Sequencing of the bound aptides yielded three highly redundant aptide sequences. The binding properties of the selected aptides, which were chemically synthesized by using a conventional solid-phase peptide synthesizer, were analyzed using a surface plasmon resonance (SPR) assay. The highest-affinity peptide, designated APT_{EDB}, exhibited an association rate constant (k_a) of approximately $1.7\times10^{4}\,M^{-1}s^{-1}$ and a dissociation rate constant (k_d) of approximately $1.1\times10^{-3}\,s^{-1}$, yielding a dissociation constant (K_d) of approximately 65 nM (Table 1 and Figure 2a). To further investigate the specificity of this aptide, we performed a phage enzyme-linked immunosorbent assay (ELISA) experiment using the corresponding APT_{EDB} phage (Figure S1c in the Supporting Information). Our results revealed that APT_{EDB} exhibited high-level binding of EDB but only negligible binding to various other non-target proteins, indicating that the aptide had high specificity for its target protein.

To determine whether aptides actually formed the pre-organized structure that we expected based on our rational design, we performed a preliminary NMR-spectroscopy-based structural analysis of APT_{EDB}. Twenty NMR structures were converged into the model aptide shown in Figure 1b. As expected, the trpzip scaffold caused APT_{EDB} to form a pre-organized hairpin structure in aqueous solution, and the two target binding sites were positioned randomly in an open-mouthed shape as well as at the same side that may be able to facilitate target binding in a fixed or defined distance (see Table S2 in the Supporting Information for details on the NMR spectroscopy analysis). Furthermore, circular dichroism spectroscopy experiments with only the trpzip scaffold and several candidate aptides revealed that aptides were able to maintain pre-organized hairpin structures as the trpzip scaffold does (Figure S2 in the Supporting Information).[14]

To further examine the cooperative binding between the two arms of the aptide's target-binding region, we synthesized APT_{EDB} derivatives with deletions of either the N- or C-terminal variable parts and measured their affinities (Figure 2b). Both the APT_{EDB} derivatives with N- and C-terminal deletions showed dramatic (at least three orders of magnitude) losses of their affinities, which dropped from 65 nM to 12 and 592 μM, respectively. These results indicate that the two target-binding regions of APT_{EDB} cooperatively bind the target molecule to give the aptide its high affinity and specificity. Next, we examined the importance of the pre-organized hairpin structure using a scaffold mutant of APT_{EDB} in which the four tryptophan residues in the trpzip scaffold were replaced with glycine, which resulted in the complete loss of hairpin structure (Figure S2 in the Supporting Information). SPR affinity measurements revealed that, unlike the parent APT_{EDB}, the scaffold mutant showed no binding to EDB at 1 μM and only weak binding even at a concentration of 100 μM (Figure 2c). Furthermore, we examined whether the structure-stabilizing, rigid trpzip scaffold improves the stability of an aptide in serum. A high-performance liquid chromatography (HPLC) analysis revealed that the half-life of APT_{EDB} was 12-fold greater than that of the scaffold mutant lacking the structure (approximately 60 min versus approximately 5 min, respectively; Figure S3 in the Supporting Information). These results clearly indicate that the trpzip scaffold is vitally important for maintaining the aptide structure with the cooperative target binding of the two arms and for improving serum stability.

The aptide selection strategy affords a unique mechanism for stepwise affinity maturation (Figure 2d). The first step in the maturation process is to maintain either the N- or C-

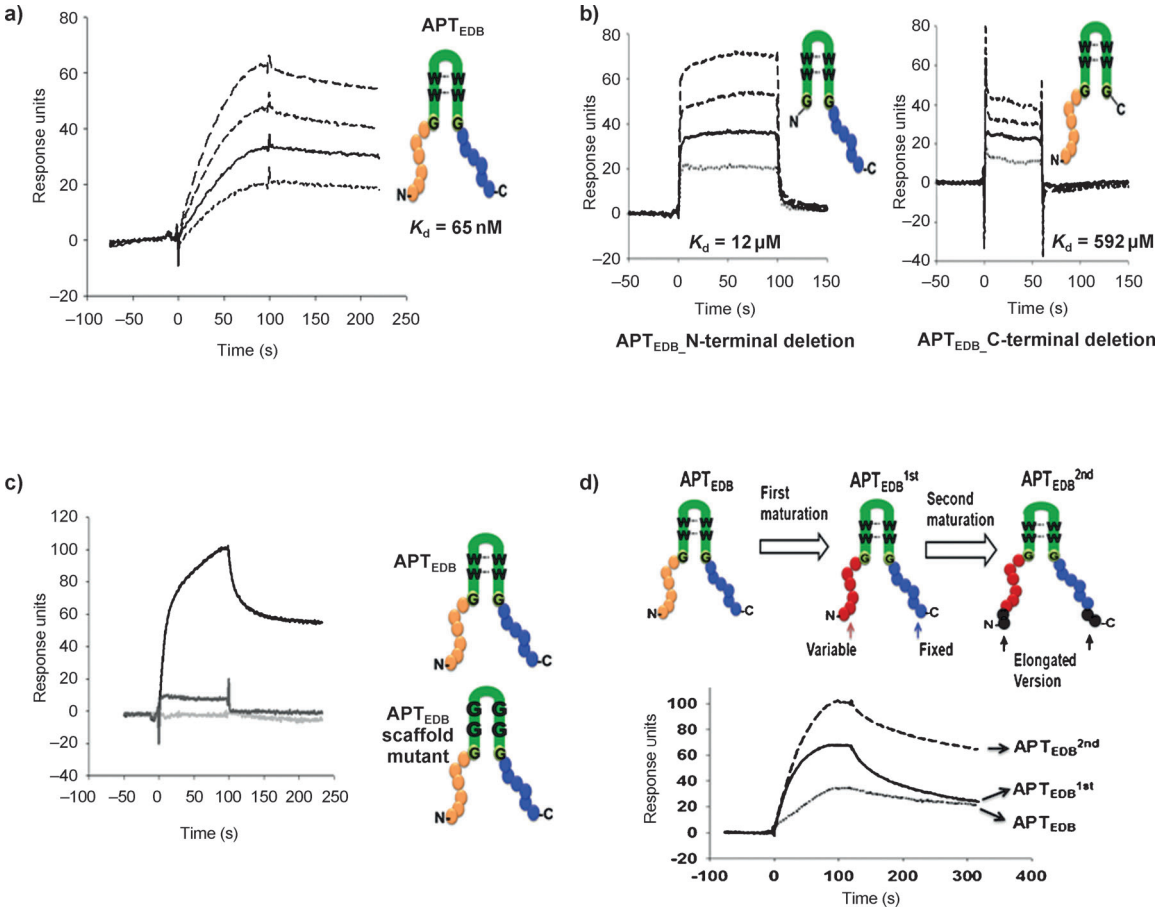

Figure 2. a) SPR sensorgrams obtained from BIAcore chips with immobilized EDB upon treatments with various concentrations of APT_{EDB} (100, 200, 400, and 600 nM). b) Affinity measurements of APT_{EDB} derivatives with deletions of the N- or C-terminal binding parts. c) Comparison of SPR sensorgrams of parental APT_{EDB} (1 μM, black line) and an APT_{EDB} scaffold mutant (1 μM, light-gray line, and 100 μM, dark-gray line). d) A stepwise affinity maturation process for the generation of higher-affinity aptides and an overlay of SPR sensorgrams obtained from the parental APT_{EDB} and the two affinity-matured aptides (APT_{EDB}^{1st} and APT_{EDB}^{2nd}) at 250 nM. N- and -C in the peptide drawings indicate the positions of the N terminus and C terminus, respectively.

terminal variable part of the aptide "hit" obtained by selection while randomizing the six amino acids of the other variable part. In the second affinity maturation step, two randomized amino acids were introduced at both the N- and C-termini of the first affinity-maturated aptide. By using this approach, we obtained new EDB-specific aptides from the 1st and 2nd affinity maturation steps, which we termed APT_{EDB}^{1st} and APT_{EDB}^{2nd}, respectively. APT_{EDB}^{2nd} exhibited approximately 20-fold better affinity (K_d ca. 3 nM) than the parent APT_{EDB} (K_d ca. 65 nM), confirming the effectiveness of the maturation step. As seen in an overlay of the SPR sensorgrams obtained using APT_{EDB}, APT_{EDB}^{1st}, and APT_{EDB}^{2nd} at 250 nM (Figure 2d), the mature aptides clearly demonstrated more rapid association kinetics.

To show that our aptide library may be used as a general source of molecules binding with high-affinity, we screened for aptides targeting several other proteins, including VEGF, CD7, and the hexa-histidine (His_6) tag. We obtained a number of target-specific aptide sequences (Table S1 in the Supporting Information). As summarized in Table 1, the selected APT_{VEGF} had an affinity of approximately 30 nM, which is the highest affinity of any reported VEGF-binding peptide (the previous highest one is the v114 peptide with a K_d of ca. 230 nM).[16] The CD7-specific aptide (APT_{CD7}) also had a strong affinity of 93 nM, which is the first reported specific peptide ligand for CD7. We also generated an aptide specific to the small peptide tag, His_6-tag. The affinity of $ATP_{His\text{-}tag}$, even before affinity maturation, was approximately 71 nM, which is better than that of commercially available anti-His-tag antibody (ca. 340 nM).[17] The fact that the selected "hit" aptides for various targets exhibit double-digit nanomolar affinities even before affinity maturation indicates that our aptide platform could be used as a general source of a high-affinity peptide library.

We finally investigated whether our selected EDB-specific aptide could target EDB-expressing tumors in an in vivo model. The human glioblastoma (U87MG)-xenografted mouse tumor model was used, because it exhibits high-level EDB expression, as reported[18] and confirmed herein by using an anti-EDB antibody (Figure S4a in the Supporting Information). Tissue-level histofluorescence experiments showed that fluorescein isothiocyanate (FITC)-labeled APT_{EDB} specifically stained EDB protein in the ex vivo U87MG tissue sample in a manner similar to that of

an anti-EDB antibody, which was used as a positive control (Figure S4b in the Supporting Information). For in vivo imaging, we utilized APT_{EDB}^{1st} and scrambled aptide (scr-APT; a negative control) both labeled with the fluorescent dye Cy5.5 (Figure S5 in the Supporting Information). In vivo fluorescence images of whole animals were obtained 0, 1, 2, 4, and 6 h after intravenous injection of each dye-labeled aptide (1 nmol; Figure 3a). Notably, the fluorescence signal increased over time within the tumor for APT_{EDB}^{1st}, whereas scr-APT was not preferentially taken up into the tumor at any time point, indicating that the aptide specifically accumulated at the tumor site. After six hours, mice were sacrificed and organ and tumor samples were excised and imaged (Figure 3b). We found that APT_{EDB}^{1st} was predominantly taken up by the U87MG tumor and not by the organs (kidney, liver, lung, heart, and spleen). In contrast, scr-APT did not accumulate in the tumor. Furthermore, APT_{EDB}^{1st} did not accumulate in an LNCaP-derived prostate tumor model that lacked EDB expression (Figures S6a and S6b in the Supporting Information), thus indicating the specificity of the aptide. These results clearly demonstrate that the EDB-specific aptide could specifically bind its target in vivo, suggesting that it could prove useful as a targeting ligand for diagnostic and therapeutic applications in vivo.

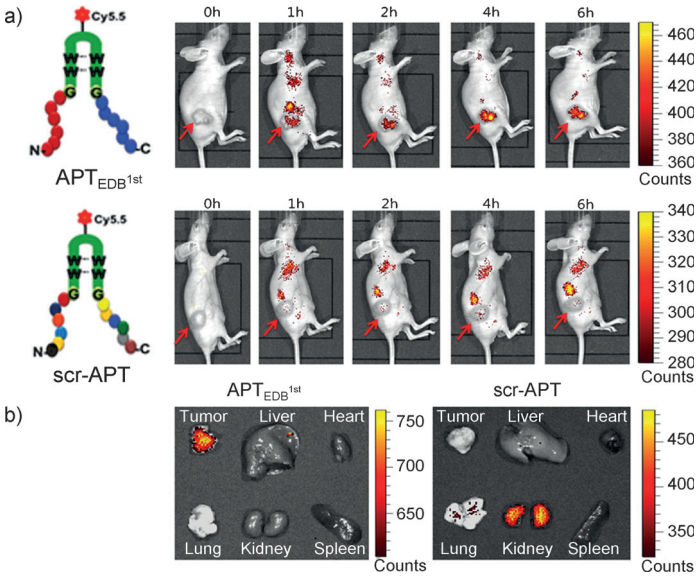

Figure 3. a) Tumor targeting of the EDB-specific aptide in a human glioblastoma xenograft mouse model. In vivo fluorescence imaging of subcutaneous U87MG glioblastoma-tumor-bearing athymic nude mice after intravenous injection of Cy5.5-labeled APT_{EDB}^{1st} or Cy5.5-labeled scrambled aptide (scr-APT). Near-IR (NIR) fluorescence images were acquired at 0, 1, 2, 4, 6 h, and the results were normalized with respect to the image taken at one hour. The red arrow indicates the position of the tumor. b) Representative images of organs dissected from tumor-bearing mice sacrificed six hours after intravenous injection of Cy5.5-labeled APT_{EDB}^{1st} or Cy5.5-labeled scr-APT. N- and -C in the peptide drawings indicate the positions of the N terminus and C terminus, respectively.

The proof-of-concept studies reported herein show that we have developed a novel class of high-affinity peptides for potential biological and biomedical uses. Aptides have several advantages over larger high-affinity molecules. First, with 26 amino acids (ca. 3 kDa), aptides can be synthesized in a single chemical process; they are also much smaller than current leading molecules that bind to a specific target, such as antibodies (ca. 150 kDa), aptamers (>10 kDa), and protein scaffolds (ca. 7–20 kDa). It has been shown that smaller molecules lead to higher accumulation in tumor tissue than larger molecules with similar affinities because of fast extravasation and high diffusibility in tumor tissues, in case the sizes of both molecules are below a molecular weight cut-off (ca. 40 kDa) for elimination through kidneys; in this application, higher affinity may result in better tumor uptake.[5] Thus aptides may be appropriate candidates for tumor imaging and therapy, because they are small, high-affinity peptides with affinities in the nanomolar range with slow dissociation rates. Second, unlike antibodies or proteins, aptides are amenable to site-specific conjugation to a variety of molecules (e.g., drugs and imaging modalities) during peptide synthesis, thereby expanding the range of potential applications.[19] Lastly, aptides showed no unintended immune responses under our experimental conditions (Figure S7 in the Supporting Information); thus, they may exhibit lower toxicities than many other biological agents. Taken together, the potential applications of our novel aptide technology span the full range of biopharmaceutical applications, from biological research and diagnostics to therapeutics, including the direct development of peptide drugs.

Received: November 9, 2011
Revised: December 12, 2011
Published online: January 24, 2012

Keywords: aptides · imaging agents · peptides · peptide design · phage display

[1] a) J. M. Reichert, C. J. Rosensweig, L. B. Faden, M. C. Dewitz, *Nat. Biotechnol.* **2005**, *23*, 1073–1078; b) P. J. Carter, *Nat. Rev. Immunol.* **2006**, *6*, 343–357.
[2] a) T. T. Hansel, H. Kropshofer, T. Singer, J. A. Mitchell, A. J. T. George, *Nat. Rev. Drug Discovery* **2010**, *9*, 325–338; b) S. Kozlowski, P. Swann, *Adv. Drug Delivery Rev.* **2006**, *58*, 707–722; c) G. M. Thurber, M. M. Schmidt, K. D. Wittrup, *Adv. Drug Delivery Rev.* **2008**, *60*, 1421–1434.
[3] a) C. Grönwall, S. Stahl, *J. Biotechnol.* **2009**, *140*, 254–269; b) M. Gebauer, A. Skerra, *Curr. Opin. Chem. Biol.* **2009**, *13*, 245–255.
[4] a) E. Dausse, S. D. R. Gomes, J.-J. Toulme, *Curr. Opin. Pharmacol.* **2009**, *9*, 602–607; b) G. Mayer, *Angew. Chem.* **2009**, *121*, 2710–2727; *Angew. Chem. Int. Ed.* **2009**, *48*, 2672–2689.
[5] a) C. Zahnd, M. Kawe, M. T. Stumpp, C. d. Pasquale, R. Tamaskovic, G. N. Davidescu, B. Dreier, R. Schibli, H. K. Binz, R. Waibel, A. Plückthun, *Cancer Res.* **2010**, *70*, 1595–1605; b) M. M. Schmidt, K. D. Wittrup, *Mol. Cancer Ther.* **2009**, *8*, 2861–2871.
[6] a) S. Maschauer, J. Einsiedel, R. Haubner, C. Hocke, M. Ocker, H. Hubner, T. Kuwert, P. Gmeiner, O. Prante, *Angew. Chem.* **2010**, *122*, 988–992; *Angew. Chem. Int. Ed.* **2010**, *49*, 976–979; b) K. Wang, S. Purushotham, J.-Y. Lee, M.-H. Na, H. Park, S.-J. Oh, R.-W. Park, J. T. Park, E. Lee, B. C. Cho, M.-N. Song, M.-C. Baek, W. Kwak, J. Yoo, A. S. Hoffman, Y.-K. Oh, I.-S. Kim, B.-H. Lee, *J. Controlled Release* **2010**, *148*, 283–291; c) I. U. Khan, D.

Zwanziger, I. Bohme, M. Javed, H. Naseer, S. W. Hyder, A. G. Beck-Sickinger, *Angew. Chem.* **2010**, *122*, 1174 – 1177; *Angew. Chem. Int. Ed.* **2010**, *49*, 1155 – 1158; d) S. Lee, J. Xie, X. Chen, *Biochemistry* **2010**, *49*, 1364 – 1376.

[7] P. Vlieghe, V. Lisowski, J. Martinez, M. Khrestchatisky, *Drug Discovery Today* **2010**, *15*, 40 – 56.

[8] H. Kolmar, *Curr. Opin. Pharmacol.* **2009**, *9*, 608 – 614.

[9] P. M. Watt, *Nat. Biotechnol.* **2006**, *24*, 177 – 183.

[10] a) J. Lehtio, T. T. Teeri, P. A. Nygren, *Proteins Struct. Funct. Genet.* **2000**, *41*, 316 – 322; b) G. P. Smith, S. U. Patel, J. D. Windass, J. M. Thornton, G. Winter, A. D. Griffiths, *J. Mol. Biol.* **1998**, *277*, 317 – 332; c) P. M. Watt, *Future Med. Chem.* **2009**, *1*, 257 – 265.

[11] a) C. Souriau, L. Chiche, R. Irving, P. Hudson, *Biochemistry* **2005**, *44*, 7143 – 7155; b) A. P. Silverman, A. M. Levin, J. L. Lahti, J. R. Cochran, *J. Mol. Biol.* **2009**, *385*, 1064 – 1075.

[12] N. L. Daly, R. J. Clark, D. J. Craik, *J. Biol. Chem.* **2003**, *278*, 6314 – 6322.

[13] T. E. Ellenberger, C. J. Brandl, K. Struhl, S. C. Harrison, *Cell* **1992**, *71*, 1223 – 1237.

[14] A. G. Cochran, N. J. Skelton, M. A. Starovasnik, *Proc. Natl. Acad. Sci. USA* **2001**, *98*, 5578 – 5583.

[15] M. Kaspar, L. Zardi, D. Neri, *Int. J. Cancer* **2006**, *118*, 1331 – 1339.

[16] a) S. A. Kenrick, P. S. Daugherty, *Protein Eng. Des. Sel.* **2010**, *23*, 9 – 17; b) W. J. Fairbrother, H. W. Christinger, A. G. Cochran, G. Fuh, C. J. Keenan, C. Quan, S. K. Shriver, J. Y. K. Tom, J. A. Wells, B. C. Cunningham, *Biochemistry* **1998**, *37*, 17754 – 17764.

[17] K. M. Müller, K. M. Arndt, K. Bauer, A. Plü ckthun, *Anal. Biochem.* **1998**, *259*, 54 – 61.

[18] G. Mariani, A. Lasku, E. Balza, B. Gaggero, C. Motta, L. D. Luca, A. Dorcaratto, G. A. Viale, D. Neri, L. Zardi, *Cancer* **1997**, *80*, 2378 – 2384.

[19] a) J. M. Chan, L. Zhang, R. Tong, D. Ghosh, W. Gao, G. Liao, K. P. Yuet, D. Gray, J.-W. Rhee, J. Cheng, G. Golomb, P. Libby, R. Langer, O. C. Farokhzad, *Proc. Natl. Acad. Sci. USA* **2010**, *107*, 2213 – 2218; b) R. Mahato, W. Tai, K. Cheng, *Adv. Drug Delivery Rev.* **2011**, *63*, 659 – 670.

